

DESIGN OF NOVEL RECONFIGURABLE FREQUENCY SELECTIVE SURFACES WITH TWO CONTROL TECHNIQUES

Khaled ElMahgoub^{1, *}, Fan Yang^{1, 2}, and Atef Z. Elsherbeni¹

¹Center of Applied Electromagnetic System Research (CAESR), Department of Electrical Engineering, University of Mississippi, Mississippi, USA

²Department of Electronic Engineering, Tsinghua University, Beijing 100084, China

Abstract—Novel reconfigurable frequency selective surfaces (RFSS) are designed using a finite-difference time-domain with periodic boundary condition (FDTD/PBC) algorithm. The FSS are reconfigured using two techniques: the first technique providing a wide frequency tuning range is based on using diodes to change the current distribution over the FSS surface, and the second technique exhibiting a finer frequency tuning resolution is based on changing the grid orientation of the FSS mechanically. Simulation results are provided to validate the concept of RFSS. The results show that these designs provide a wide dynamic range of reconfigurability and a large degree of freedom in controlling the FSS frequency response.

1. INTRODUCTION

There has been a significant amount of interest in frequency selective surfaces (FSS) over the years, as it has been investigated for a variety of applications, such as electromagnetic (EM) filters, radomes, absorbers, electromagnetic band gap, and many other applications [1]. In most of the FSS applications, the geometry and material parameters have been designed to produce a static frequency response. However, several groups have investigated the possibility of tuning or reconfiguring an

Received 28 September 2012, Accepted 12 December 2012, Scheduled 19 December 2012

* Corresponding author: Khaled ElMahgoub (kelmahgoub@ieee.org).

FSS so that its frequency response can be shifted or altered while in operation [2–7]. This can be accomplished either by changing the electromagnetic properties of the FSS substrate, or by altering the geometry of the structure, or by introducing circuit elements into the FSS screen that vary the current flow between metallic patches. In the first class of reconfigurable FSS (RFSS), the frequency response of the FSS is changed by altering the electromagnetic properties of the substrate, which can be accomplished by many means such as using ferrite as the substrate material and applying DC bias across it, or by using a liquid dielectric as a substrate and change its volume [2]. The second RFSS class is based on changing the geometry of the FSS mechanically by using motors, micro-electro-mechanical systems (MEMS) technology, etc.. The metallic elements of the FSS are designed to be able to change orientation or position which will change the frequency response of the FSS. The third class of RFSS to be considered, incorporates circuit components into the metallic screen that can be used to vary the current between metallic elements which in turns change the frequency response of the FSS [3].

In this paper, two techniques are used to design a novel RFSS. The first technique is based on using a diode between the metallic parts of the FSS elements. The diode is switched between two states (ON and OFF) to change the frequency response of the FSS by varying the current flow. The second technique is based on changing the grid arrangement of the FSS elements mechanically from axial to skewed grid with different skew angles. In [8] it was proven that changing the grid of the FSS changes its frequency response and the FDTD results were confirmed by frequency domain simulation results. The design and the analysis are done using the FDTD/PBC algorithm described in [8], which is based on the constant horizontal wavenumber approach [9–15]. The diode is simulated using the actual diode current-voltage equation for forward bias, while using a circuit model consisting of resistor and capacitor in parallel for reversed bias in the presence of both axial and skewed FSS grids, which provides more accurate simulation results compared to simulating the diode as an open circuit (OC) for the OFF state and a short circuit (SC) for the ON state [16]. However, some other circuit models could be used to account for other parasitic elements of the diode and its insertion loss. Numerical results are provided to prove the validity of the design.

The paper is organized as follows: In Section 2, two designs of different RFSS structures are described. In Section 3, numerical results showing the validity of these new design are provided. In Section 4, conclusions are provided.

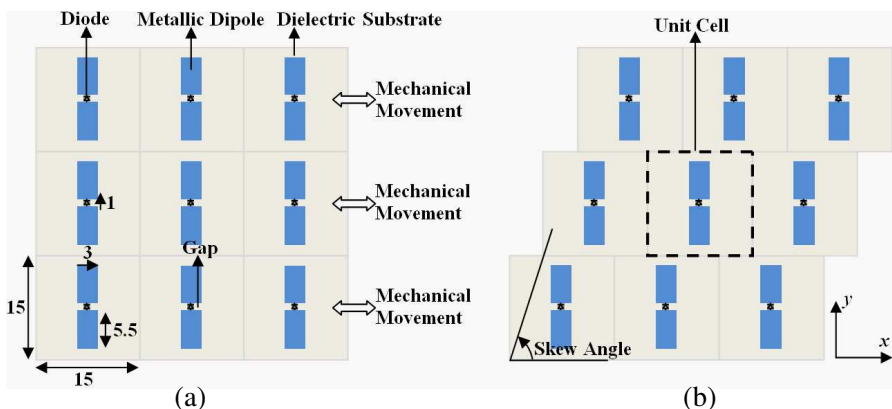


Figure 1. The geometry of the proposed dipole RFSS, (a) axial case, (b) skewed grid case. (all dimensions are in mm).

2. THE PROPOSED DESIGNS

In this section two novel RFSS structures are described using the new design technique.

2.1. Dipole FSS

The first RFSS structure consists of dipole elements. The basic geometrical dimensions of the dipole are: length 12 mm, width 3 mm, and gap 1 mm (the gap is used for mounting the diode). The periodicity is 15 mm in both x - and y -directions as shown in Figure 1. The substrate has a thickness of 6 mm and a relative permittivity $\epsilon_r = 2.2$. As shown in Figure 1, the FSS has two control parameters that increase the degree of freedom of the reconfigurability. The first control parameter is the diode that has two states, ON or OFF. The diode acts as a short circuit connecting the two arms of the dipole in the ON state, while in the OFF state it acts as an open circuit. Due to these two states the current distribution on the dipoles will change from one state to the another, leading to changes in the frequency response. The advantage of using the FDTD/PBC is to implement the diode using the actual diode current-voltage Equation (1) in the forward bias case and a circuit model consisting of a 50 k Ω resistor and 0.025 pF capacitor in parallel, this model is based on MA4GP907 PIN diode [17]. The diode current is characterized by voltage-current relation as shown in [16] that is;

$$I_d = I_0 \left[e^{(qV_d/kT)} - 1 \right], \tag{1}$$

where q is the absolute value of the electron charge in Coulombs, k the Boltzmann's constant, I_0 the saturation current of the diode, and T the temperature in Kelvin. The values used in the simulations are as follows: $q = 1.602e-19$ C, $k = 1.38066e-23$, $T = 300$ K, $I_0 = 1e-14$ A. The diode implementation procedure provided in [16] is used to simulate the diode in the FDTD/PBC algorithm.

The second control parameter is the movements of different rows of the FSS as shown in Figure 1(b). These mechanical movements can be performed, for example using a stepper motor or for smaller designs MEMS structure. The movements will change the grid orientation of the FSS, which in turn will affect the frequency response of the FSS. According to [8], different skew angles give frequency shift for the frequency response of the FSS.

2.2. Square Patch with Slot FSS

The second RFSS structure consists of slotted square patches. The square patch has a side of 10 mm, while the slot dimensions are 8×1 mm and the slot is centered in the square patch. In addition, the diode is mounted in the middle of the slot. The unit cell periodicity is 15 mm in both x - and y -directions as shown in Figure 2. The substrate has a thickness of 6 mm, a relative permittivity $\epsilon_r = 2.2$, and electric conductivity $\sigma_e = 0.005$ S/m. As shown in Figure 2, similar to previous case, the FSS has two control parameters that increase the degree of freedom of the reconfigurability. The first control parameter is the diode that has two states, ON or OFF. The diode short circuits the slot in the ON state, while in the OFF state it acts as an open circuit and

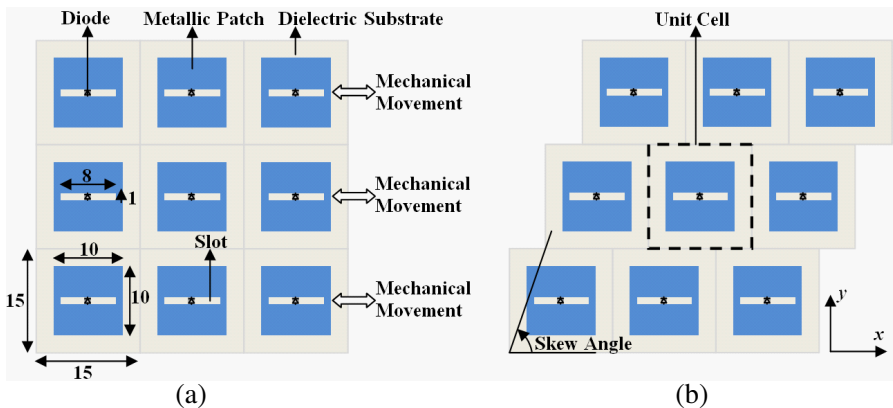


Figure 2. The geometry of the proposed square patch with slot RFSS, (a) axial case, (b) skewed grid case. (all dimensions are in mm).

the slot detours the current path and change the resonant frequency of the square patch [18]. Due to these two states the current distribution on the square patch will change from one state to another, leading to changes in the frequency response. The second control parameter is the movements of different rows of the FSS as shown in Figure 2(b). The movements will change the grid orientation of the FSS that in turn will affect the frequency response of the FSS.

3. NUMERICAL RESULTS

In this section, full-wave EM simulations are performed using the FDTD method with the diode model presented by Equation (1) to simulate different RFSS configurations. The algorithm developed in [8] is used to simulate the structure with different skew angles. The accuracy of the algorithm was confirmed through the good agreements with frequency domain results and analytical results. To completely study the proposed RFSSs different configurations are simulated. The FDTD code was developed using MATLAB [19] and run on a computer with an Intel Core i7 CPU Q720, 1.6 GHz with 6 GB RAM. As shown in Tables 1 and 2, the two structures are illuminated by both normal and oblique incident plane waves, the two states of the diode are studied and different values of skew angles are used.

3.1. Dipole FSS

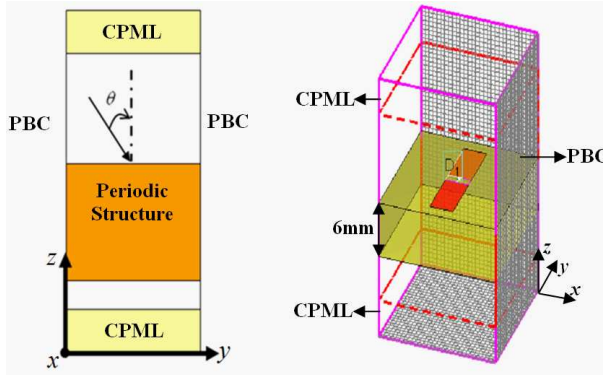
The dipole FSS structure is excited by a transverse electric (TE^z) plane wave using cosine modulated Gaussian pulse centered at 8 GHz with

Table 1. Different simulation parameters for dipole FSS designs.

Case No.	Diode State	Skew Angle	Incident k_x, k_y (m^{-1})	Position of Reflection Coefficient Peak
1	OFF	90°	Normal $k_x = k_y = 0$	12.79 GHz
2	ON	90°	Normal $k_x = k_y = 0$	7.53 GHz
3	OFF	68.19°	Normal $k_x = k_y = 0$	13.71 GHz
4	ON	68.19°	Normal $k_x = k_y = 0$	7.83 GHz
5	OFF	90°	Oblique $k_x = 20, k_y = 0$	12.7 GHz
6	ON	90°	Oblique $k_x = 20, k_y = 0$	7.54 GHz
7	OFF	68.19°	Oblique $k_x = 20, k_y = 0$	13.65 GHz
8	ON	68.19°	Oblique $k_x = 20, k_y = 0$	7.84 GHz

Table 2. Different simulation parameters for square patch with slot FSS designs.

Case No.	Diode State	Skew Angle	Incident k_x, k_y (m^{-1})	Position of Reflection Coefficient Peak
1	OFF	90°	Normal $k_x = k_y = 0$	10.04 GHz
2	ON	90°	Normal $k_x = k_y = 0$	12.96 GHz
3	OFF	63.43°	Normal $k_x = k_y = 0$	10.07 GHz
4	ON	63.43°	Normal $k_x = k_y = 0$	13.08 GHz
5	OFF	90°	Oblique $k_x = 8, k_y = 2$	10.09 GHz
6	ON	90°	Oblique $k_x = 8, k_y = 2$	12.99 GHz
7	OFF	63.43°	Oblique $k_x = 8, k_y = 2$	10.12 GHz
8	ON	63.43°	Oblique $k_x = 8, k_y = 2$	13.11 GHz

**Figure 3.** FDTD simulation domain for dipole FSS.

a bandwidth of 16 GHz for normal incident case ($k_x = k_y = 0 \text{ m}^{-1}$). The bandwidth in this paper is defined as the frequency band where the magnitude of the frequency domain reaches 10% of its maximum. While for oblique incident case ($k_x = 20 \text{ m}^{-1}$, $k_y = 0 \text{ m}^{-1}$) (for minimum frequency of 2 GHz), the structure is excited using cosine modulated Gaussian pulse centered at 8.5 GHz with a bandwidth of 15 GHz. As shown in Figure 3, the top and bottom boundaries of the computational domain are terminated by the convolutional perfect matched layer (CPML) as presented in [16]. The FDTD grid cell size is $\Delta x = \Delta y = \Delta z = 0.5 \text{ mm}$ and 3,000 time steps are used. The computational time for the FDTD code with diode implementation is 2.08 minutes and the memory usage is 0.2 MB. The result of the 90° case is compared with the results form HFSS [20] as shown in

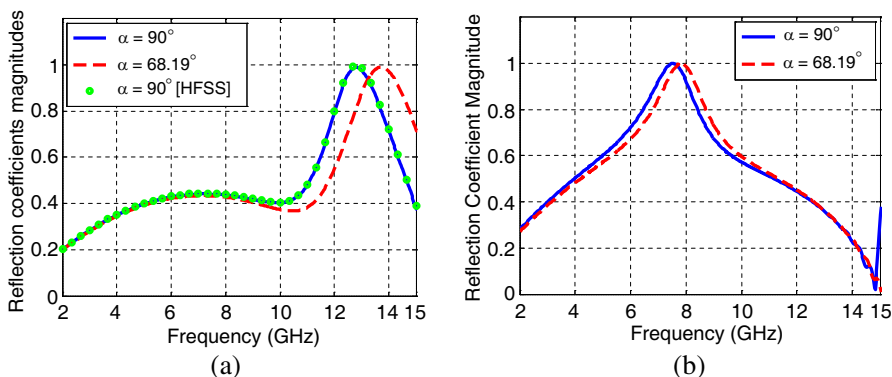


Figure 4. Normal incident ($k_x = k_y = 0 \text{ m}^{-1}$) with different skew angles for dipole FSS, (a) diode OFF, (b) diode ON.

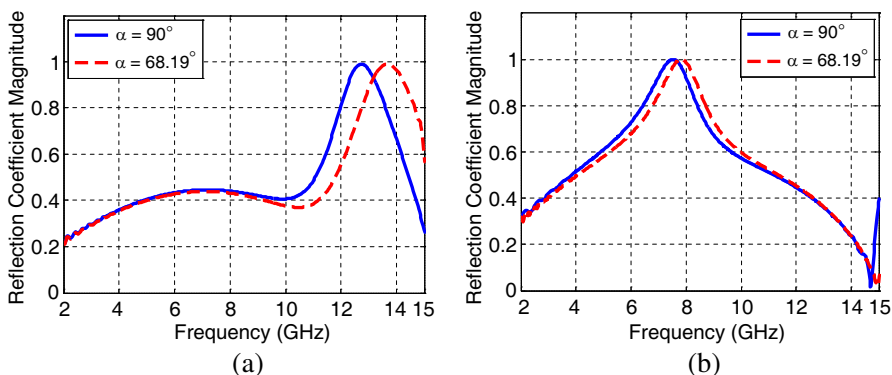


Figure 5. Oblique incident ($k_x = 20 \text{ m}^{-1}$, $k_y = 0 \text{ m}^{-1}$) with different skew angles for dipole FSS, (a) diode OFF, (b) diode ON.

Figure 4(a), the HFSS requires 35 minutes for 40 frequency points and the memory usage is 30 MB. Good agreement can be observed which proves the validity of the design, while the FDTD is more efficient in both memory usage and computational time.

From Figures 4 and 5, the changes in the frequency response can be noticed. The effects of the two configurations parameters are observed. Turning on the diode shifts the reflection coefficient peak from almost 13 GHz to 7.5 GHz. The frequency ratio is around 2 here. If another frequency ratio is preferred, one can change the position of the diode from center to a proper offset location along y -directions. In addition, changing the skew angle of the FSS grid also introduces a slight frequency shift in the reflection coefficient. The

different frequency values of the reflection coefficient peak (almost total reflection) are stated in Table 1. In summary, the new design provides two degrees of freedom in the reconfigurability. A large frequency shift can be obtained by turning on the diode, while a finer frequency shift can be obtained by changing the grid skew angle.

It is worthwhile to point out that some practical considerations should be considered when fabricating such a design. For example, the diodes biasing networking should be carefully laid out for such a large number of diodes. The second issue is the implementation of the mechanical movement and the proper control of these movements.

3.2. Square Patch with Slot FSS

The square patch with slot FSS structure is excited by a TE^z plane wave using cosine modulated Gaussian pulse centered at 8 GHz with

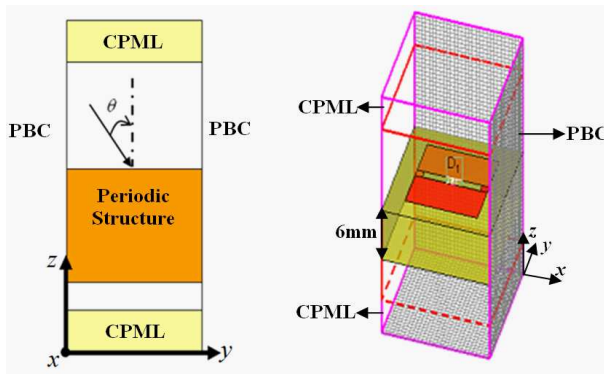


Figure 6. FDTD simulation domain for square patch with slot FSS.

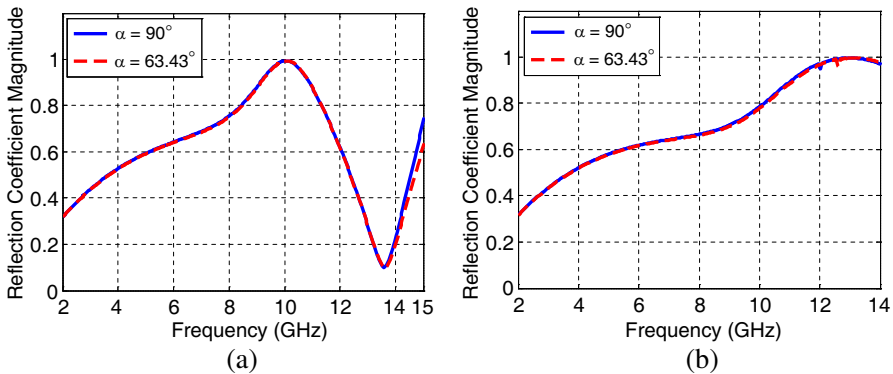


Figure 7. Normal incident ($k_x = k_y = 0 \text{ m}^{-1}$) with different skew angles for square patch with slot FSS, (a) diode OFF, (b) diode ON.

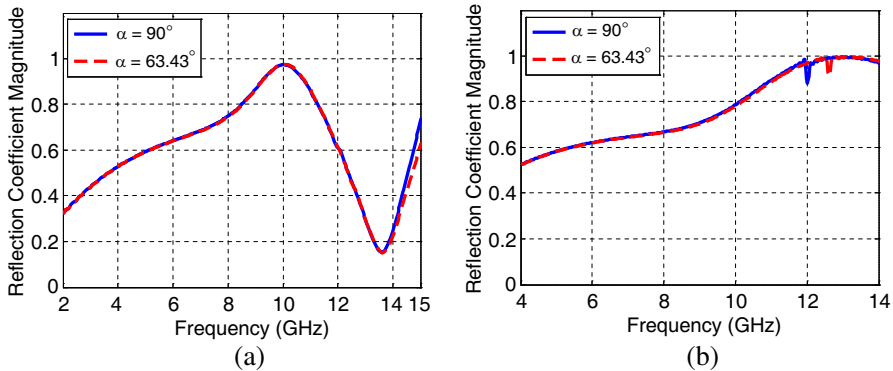


Figure 8. Oblique incident ($k_x = 8 \text{ m}^{-1}$, $k_y = 2 \text{ m}^{-1}$) with different skew angles for square patch with slot FSS, (a) diode OFF, (b) diode ON.

a bandwidth of 16 GHz for normal incident case ($k_x = k_y = 0 \text{ m}^{-1}$). While for oblique incident case ($k_x = 8 \text{ m}^{-1}$, $k_y = 2 \text{ m}^{-1}$), the structure is excited using cosine modulated Gaussian pulse centered at 10 GHz with a bandwidth of 20 GHz. As shown in Figure 6 the top and bottom boundaries of the computational domain are terminated by the convolutional perfect matched layer (CPML) as presented in [16]. The FDTD grid cell size is $\Delta x = \Delta y = \Delta z = 0.5 \text{ mm}$ and 3,000 time steps are used. The computational time for the FDTD code with diode implementation is 2.5 minutes and the memory usage is 0.22 MB. From Figures 7 and 8, the changes in the frequency response can be noticed. The effects of the two configurations parameters are observed. As shown in Figure 7, for normal incidence, turning on the diode changes the frequency response from a resonance point at 10.04 GHz to a resonance point at 12.96 GHz, similar behavior can be noticed for the oblique incidence case. In addition, changing the skew angle of the grid of the FSS introduces a slight frequency shift in the reflection coefficient, e.g., from 10.04 GHz to 10.07 GHz for normal incidence case. The different frequency values of the reflection coefficient peak are listed in Table 2. The new design provides two degrees of freedom in the reconfigurability. A large frequency shift can be obtained by turning on the diode, while a finer frequency shift can be obtained by changing the grid skew angle.

4. CONCLUSION

Novel RFSS designs were introduced in this paper. The reconfigurability of the design is based on two techniques, the first

is to control a diode state for a wide frequency tuning range and the second is to control a mechanical movement to change the skew angle of the FSS grid for a fine frequency tuning resolution. The designs were simulated using FDTD/PBC algorithm, while taking into account the actual model of the diode and different skew angles. The simulations were efficient in both memory usage and computational time. The results showed that these new designs provide a wide dynamic range of frequency reconfigurability and a large degree of freedom in controlling the FSS frequency response.

REFERENCES

1. Munk, B. A., *Frequency Selective Surfaces: Theory and Design*, Wiley, New York, 2000.
2. Chang, T. K., R. J. Langley, and E. A. Parker, "Frequency selective surfaces on biased ferrite substrates," *IEE Electronic Letter*, Vol. 30, No. 15, 1193–1194, 1994.
3. Bossard, J. A., D. H. Werner, T. S. Mayer, and R. P. Drupp, "A novel design methodology for reconfigurable frequency selective surfaces using genetic algorithms," *IEEE Transactions on Antennas and Propagation*, Vol. 53, No. 4, 1390–1400, 2005.
4. Pirhadi, A., F. Keshmiri, M. Hakkak, and M. Tayarani, "Analysis and design of dual band high directive EBG resonator antenna using square loop FSS as superstrate layer," *Progress In Electromagnetics Research*, Vol. 70, 1–20, 2007.
5. Zhang, J.-C., Y.-Z. Yin, and R. Yi, "Resonant characteristics of frequency selective surfaces on ferrite substrates," *Progress In Electromagnetics Research*, Vol. 95, 355–364, 2009.
6. Kristensson, G., M. Åkerberg, and S. Poulsen, "Scattering from a frequency selective surface supported by a bianisotropic substrate," *Progress In Electromagnetics Research*, Vol. 35, 83–114, 2002.
7. Qing, A. and C. K. Lee, "An improved model for full wave analysis of multilayered frequency selective surface with gridded square element," *Progress In Electromagnetics Research*, Vol. 30, 285–303, 2001.
8. ElMahgoub, K., F. Yang, A. Z. Elsherbeni, V. Demir, and J. Chen, "FDTD analysis of periodic structures with arbitrary skewed grid," *IEEE Transactions on Antennas and Propagation*, Vol. 58, No. 8, 2649–2657, 2010.
9. Aminian, A., F. Yang, and Y. Rahmat-Samii, "Bandwidth determination for soft and hard ground planes by spectral FDTD:

- A unified approach in visible and surface wave regions,” *IEEE Transactions on Antennas and Propagation*, Vol. 53, No. 1, 18–28, 2005.
10. ElMahgoub, K., F. Yang, A. Z. Elsherbeni, V. Demir, and J. Chen, “FDTD analysis of periodic structures with arbitrary skewed grid,” *Proc. IEEE Antennas and Propagation Society International Symposium*, 2010.
 11. ElMahgoub, K., F. Yang, and A. Z. Elsherbeni, “Design and analysis of reconfigurable frequency selective surfaces using FDTD,” *Procedures of the Applied Computational Electromagnetics Society*, 2011.
 12. Yang, F., J. Chen, R. Qiang, and A. Z. Elsherbeni, “A simple and efficient FDTD/PBC algorithm for scattering analysis of periodic structures,” *Radio Sci.*, Vol. 42, RS4004, Jul. 2007.
 13. ElMahgoub, K., F. Yang, and A. Z. Elsherbeni, “FDTD/GSM analysis of multilayered periodic structures with arbitrary skewed grid,” *IEEE Transactions on Microwave Theory and Techniques*, Vol. 59, No. 12, 3264–3271, 2011.
 14. ElMahgoub, K., F. Yang, A. Z. Elsherbeni, V. Demir, and J. Chen, “Analysis of multilayered periodic structures using a hybrid FDTD/GSM method,” *IEEE Antennas and Propagation Magazine*, Vol. 54, No. 2, 57–73, 2012.
 15. ElMahgoub, K., A. Z. Elsherbeni, and F. Yang, “Dispersive periodic boundary conditions for finite-difference time-domain method,” *IEEE Transactions on Antennas and Propagation*, Vol. 60, No. 4, 2118–2122, 2012.
 16. Elsherbeni, A. and V. Demir, *The Finite Difference Time Domain Method for Electromagnetics: With MATLAB Simulations*, SciTech Publishing, 2009.
 17. Data Sheet of MA4GP907 GaAs Flip Chip PIN, <http://www.macomtech.com/datasheets/MA4GP907.pdf>.
 18. Yang, F. and Y. Rahmat-Samii, “Patch antenna with switchable slots (PASS) in wireless communications: Concepts, designs, and applications,” *IEEE Antennas and Propagation Magazine*, Vol. 47, No. 2, 13–29, 2005.
 19. MATLAB distributed by mathworks, www.mathworks.com.
 20. HFSS Software is distributed by the ANSYS Corporation: <http://www.ansys.com/>.